Ultrasound in Med. & Biol., Vol. 46, No. 1, pp. 1–10, 2020

0301-5629/$ - see front matter

https://doi.org/10.1016/j.ultrasmedbio.2019.08.008

● *Original Contribution*

POINT-OF-CARE ULTRASOUND—A NEW OPTION FOR EARLY QUANTITATIVE ASSESSMENT OF PULMONARY EDEMA

ZHIXING ZHU,* XIHUA LIAN,† YIMING ZENG,* WEIJING WU,* ZHIRONG XU,† YONGJIAN CHEN,† JINGYUN LI,‡ XIAOSHAN SU,* LIQING ZENG,§ and GUORONG LV†,‡

* Department of Pulmonary and Critical Care Medicine, Second Affiliated Hospital of Fujian Medical University, Respirology Medicine Centre of Fujian Province, Fujian, China; † Department of Ultrasound Medicine, Second Affiliated Hospital of Fujian Medical University; ‡ Collaborative Innovation Center for Maternal and Infant Health Service Application Technology, Quanzhou Medical College, Quanzhou City Luoyang River, China; and § Department of Ultrasound Medicine, Maternal and Child Health Hospital of Fujian Province, Fujian, China

(*Received* 21 *December* 2018; *revised* 20 *June* 2019; *in final from* 5 *August* 2019)

Abstract—The aim of the work described here was to investigate the value of point-of-care ultrasound (POCUS) in the early assessment of the severity of pulmonary edema in rabbits. A rabbit oleic acid (OA)-induced pulmonary edema model was used. Thirty-two New Zealand rabbits were randomly divided into four groups: a control group and three pulmonary edema groups (mild, moderate and severe). Features of transthoracic B-line artifacts (BLA), blood pH, PaO_2 and $PaCO_2$, serum inflammatory factors, lung coefficient (LC), lung wet-to-dry weight ratio (W/D) and lung histopathology were assessed. BLA features and severity of pulmonary edema were semi-quantitatively scored. Correlations between the number of BLA and PaO_2, $PaCO_2$, serum inflammatory factors, LC and W/D were analyzed. An additional 8 rabbits with severe pulmonary edema were used as the verified group, in which the lung was divided into *ex vivo* BLA (BLA-ev)-free (BLA-ev-free) and BLA-ev-clustered subregions depending on the features of BLA-ev recorded by *ex vivo* lung ultrasound. Lung specimens from each subregion were collected for histopathological examination. Relationships between features of BLA-ev and lung histopathological abnormalities were analyzed. With increasing doses of OA, number of BLA, W/D and levels of serum inflammatory factors decreased. Meanwhile, lung pathologic abnormalities were aggravated. In addition, time of appearance of BLA, blood pH and PaO_2, and $PaCO_2$ decreased dose dependently on OA ($p < 0.05$). Number of BLA was linear positively correlated with severity of pulmonary edema ($r = 0.953$, $p < 0.05$). Consistently, the features of BLA-ev reflected the severity of lung histopathological abnormalities ($r = 0.936$, $p < 0.05$). Thus, POCUS is useful in the early quantitative assessment of the severity of pulmonary edema. (E-mail: lgr_feus@sina.com) © **2019 The Author(s). Published by Elsevier Inc. on behalf of World Federation for Ultrasound in Medicine & Biology. This is an open access article under the CC BY-NC-ND license. (http://creativecommons.org/licenses/by-nc-nd/4.0/).**

Key Words: **Pulmonary edema, Early quantitative assessment, Point-of-care ultrasound, B-line artifacts.**

INTRODUCTION

Pulmonary edema is a common and life-threatening complication of many lung diseases, in which the condition changes rapidly and mortality is extremely high (Ware and Matthay 2005). Quantitative assessment of the severity of pulmonary edema is associated with clinical outcomes and prognosis (Warren et al. 2018) and may provide valuable guidance in the selection of a therapeutic strategy (Assaad et al. 2018). Mortality from pulmonary edema decreased significantly after rapid and effective treatment, which depends on early quantitative diagnosis. Therefore, accurate and early quantitative assessment has a great impact on the prognosis of pulmonary edema. Currently, the diagnosis of pulmonary edema relies on chest X-ray or computed tomography scan (Lindholm et al. 2018; Warren et al. 2018) and pulmonary artery occlusion pressure and pulmonary extravascular fluid measurement (Harvey et al. 2005). However, these methods are inaccurate, invasive and insensitive and involve exposure to radiation (Ware and Matthay 2005). Point-of-care ultrasound (POCUS) can be performed at any time and plays an important role in the diagnosis and

Address correspondence to: Guorong Lv, Department of Ultrasound, Second Affiliated Hospital of Fujian Medical University, 34 Zhongshan North Road, Quanzhou 362000, China. E-mail: lgr_feus@sina.com

monitoring of various diseases. Many lung artifacts have been well-documented; thus, POCUS has been applied to the identification of pneumothorax, pleural effusion, pneumonia and pulmonary edema (McLario and Sivitz 2015; Campbell 2018). Today, POCUS has gained more attention because of its diagnostic and assessment value in pulmonary edema. Transthoracic B-line artifacts (BLA) are defined as discrete laser-like, vertical, hyper-echoic reverberation artifacts that arise from the pleural line, extend to the bottom of the screen without fading and move synchronously with lung sliding (Volpicelli et al. 2012). These features of BLA can be used to assess the severity of pulmonary edema to some extent (Dietrich et al. 2016). However, the correlation between the features of BLA and the degree of lung pathologic abnormalities is still uncertain, and the correlation between the features of BLA and the severity of pulmonary edema is not clear (Volpicelli et al. 2012). Therefore, there is an urgent need to clarify the relationship between features of BLA and severity of lung pathologic abnormalities and to improve the accuracy of POCUS in assessing the severity of pulmonary edema.

Rabbit oleic acid (OA)-induced pulmonary edema has become one of the most well-established animal models of pulmonary edema (Rylander et al. 2004). Moreover, the lung histopathological abnormalities in rabbits with OA-induced pulmonary edema and human pulmonary edema patients are similar (Jambrik et al. 2010). In addition, the lung structures of rabbits could be clearly visualized by *in vivo* and *ex vivo* lung ultrasound (Soldati et al. 2014; Li et al. 2015). Therefore, the present study aimed to further evaluate the value of POCUS in the assessment of the severity of pulmonary edema by analyzing the relationship between the severity of pulmonary edema and the features of BLA using a rabbit OA-induced pulmonary edema model.

METHODS

Animals and group

The animal study protocol was reviewed and approved by the institutional review board and ethics committee of Second Affiliated Hospital of Fujian Medical University, Fuzhou, China (2017-012) and performed in accordance with the recommendations of the Helsinki Declaration of 1975. All animal handling procedures were approved by the Animal Care and Use Committee, Fujian Medical University (SYXK 2014-0003), and Institutional Animal Care and Use Committee.

Forty New Zealand rabbits (2.76−3.19 kg), purchased from Changzhou Cavens Laboratory Animal Center (License No. SCXK (Jiangsu) 2011-0003), were randomly divided into five groups: the control group, three pulmonary edema groups (mild, moderate, severe) and the verified group. The rabbits were maintained under specific pathogen-free conditions with free access to food and water for 1 wk and subjected to 12 h/12 h light/dark cycles.

Establishment of rabbit pulmonary edema model

The rabbit pulmonary edema model was established as described by Furue et al. (1999). Briefly, after fasting for 8 h, the rabbits were intubated in the left ear vein with a 24G cannula and anesthetized by intravenous injection of 2% pentobarbital sodium (30 mg/kg, Merck, Darmstadt, Germany). The rabbits were fixed to the operating table. Hair on the neck and the anterior and lateral chest was removed. Saline was injected in the control group. In the treated groups, OA (Merck) was administered by intravenous injection at 0.04 mL/kg (mild), 0.08 mL/kg (moderate), 0.12 mL/kg (severe) and 0.12 mL/kg (verified).

Point-of-care ultrasound

The ultrasound diagnosis system (HI VISION Preirus, Hitachi Limited, Tokyo, Japan) was equipped with a linear shallow probe with the following settings: 10-MHz central frequency, 1.4-cm depth of focal position, 3.3-cm depth of imaging plane and 70-dB dynamic range (EUP-L74 M, Hitachi Limited, Tokyo, Japan). After anesthesia, POCUS was performed longitudinally to record BLA features in each intercostal space along the bilateral midclavicular lines (four spaces each line) and anterior axillary lines (five spaces each line). In the regular B-mode images, the recording of BLA started immediately after injection and lasted 30 min. POCUS was performed continuously until BLA appeared; BLA was then recorded at 1-min intervals. The features of BLA were scored as noted in Table 1, a modified version of the scoring system described by Gutierrez et al. (2011).

Measurement of pH, PaO_2 and $PaCO_2$

Arterial blood was drawn 30 min after injection of OA. The pH, PaO_2 and $PaCO_2$ were determined immediately using a blood gas analyzer (COMBILINE BGA E, Eschweiler, Germany).

Measurement of serum inflammatory factors

Venous blood was drawn and centrifuged at 1500*g* for 10 min in a 4°C centrifuge (C1015, Beckman 64 R,

Table 1. Rating scale of BLA features of pulmonary edema

Grade	No. of BLA	Appearance of BLA (min)	Score
0	<5	>30	0
1	6−25	6−30	1
2	26−40	4−6	2
3	41−55	2−4	3
4	>56	<2	4

BLA = B-line artifacts.

Carlsbad, CA, USA), and the serum was collected. Concentrations of tumor necrosis factor (TNF)-α, interleukin (IL)-1β, IL-6 and IL-8 were measured using ELISA kits (DY5670, DY7464, DY7984, D8000 C, R&D Systems, Minneapolis, MN, USA) according to the manufacturer's instructions. Absorbance was read at 450 nm with a biokinetics microplate reader (RT-6000, Rayto, Shenzhen, China).

Determination of LC and W/D

After rabbits were sacrificed, the trachea was clamped at end-expiration, and the whole lung was harvested. Blood and water were removed from the lung surface The lung was weighed after the main bronchus was removed. The lung coefficient (LC) was calculated as lung tissue weight (g) /body weight (kg) × 100%.

The left lung was weighed immediately (wet weight) and then placed in a drying oven at 70˚C until the weight was stable and reweighed (dry weight). The wet weight-to-dry weight ratio (W/D) was calculated as W/D = wet weight/dry weight.

Histologic analysis

The right lung was used for histologic studies. For each rabbit (not including the verified group), a 0.5-cm slice starting from the upper edge of the hilum and another 0.5-cm slice in the middle of the lung were harvested and fixed in 4% paraformaldehyde for 48 h, dehydrated and embedded in paraffin; 4-μm-thick sections were prepared and processed for standard hematoxylin and eosin (H&E) staining.

For the verified group, the trachea and lung were harvested together, keeping the lung inflated by injecting air into it with a syringe. Features of *ex vivo* BLA (BLA-ev) were recorded by *ex vivo* lung ultrasound; the imaging parameters were the same as for *in vivo* transthoracic ultrasound described above. Lung tissue was divided, on the basis of BLA-ev features as described by Soldati et al. (2012), into four subregions: BLA-ev-free (≤3 BLA-ev), BLA-ev-rare-clustered (from 4−9 BLA-ev), BLA-ev-dense-clustered (>9 BLA-ev) and BLA-ev-confluent-clustered subregion (white lung). Lung specimens were harvested from each subregion, and H&E staining was performed. Thereafter, the sections were observed under an optical microscope.

Table 2. System for scoring lung tissue histopathological abnormalities

Grade	Pathologic change in lung tissue	Score
0	Normal	0
1	Neutrophil infiltration and hemorrhage in alveoli and interstitial space; edema fluid in alveolar cavity; atelectasis; necrosis (<25%)	1
2	Neutrophil infiltration and hemorrhage in alveoli and interstitial space; edema fluid in alveolar cavity; atelectasis; necrosis (25%−50%)	2
3	Neutrophil infiltration and hemorrhage in alveoli and interstitial space; edema fluid in alveolar cavity; atelectasis; necrosis (50%−75%)	3
4	Neutrophil infiltration and hemorrhage in alveoli and interstitial; edema fluid in alveolar cavity; atelectasis; necrosis (75%)	4

The severity of histopathological manifestations of pulmonary edema was assessed independently by two pathologists blinded to the treatment group, using a semiquantitative scoring system as described by Mrozek et al. (1997). The pathologic changes evaluated included alveolar and interstitial inflammation, alveolar and interstitial hemorrhage, edema, atelectasis and necrosis. These pathologic changes were independently scored on a 4-point scale as described in Table 2. The maximum possible score was 28. The average of the scores from the two pathologists was considered the final score of each subject.

Pulmonary edema severity scoring

Severity of pulmonary edema was assessed using a semiquantitative scoring system comprising pH, PaO_2, $PaCO_2$, TNF-α, IL-1 β, IL-6, IL-8, LC and W/D. Each variable was scored on a 3-point scale as described in Table 3. The maximum possible score was 27.

STATISTICAL ANALYSIS

Statistical analysis was performed with SPSS Version 17.0 (IBM, Armonk, NY, USA). Data are expressed

Table 3. Scale for rating the clinical severity of pulmonary edema

Artery blood gas analysis			Inflammatory factor in serum (pg/mL)				LC	W/D	Score
pH	PaO_2	$PaCO_2$	TNF-α	IL-1 β	IL-6	IL-8			
≥7.4	≥90	≥40	<40	<5	<15	<0	<4.0	<3.5	0
<7.4	<90	<40	<80	<10	<30	<100	<5.5	<4.5	1
<7.35	<82	<34	<160	<20	<60	<200	<6.0	<5.0	2
<7.25	<70	<30	≥160	≥20	≥60	≥200	≥6.0	≥5.0	3

LC = lung coefficient; W/D = wet weight-to-dry weight ratio.

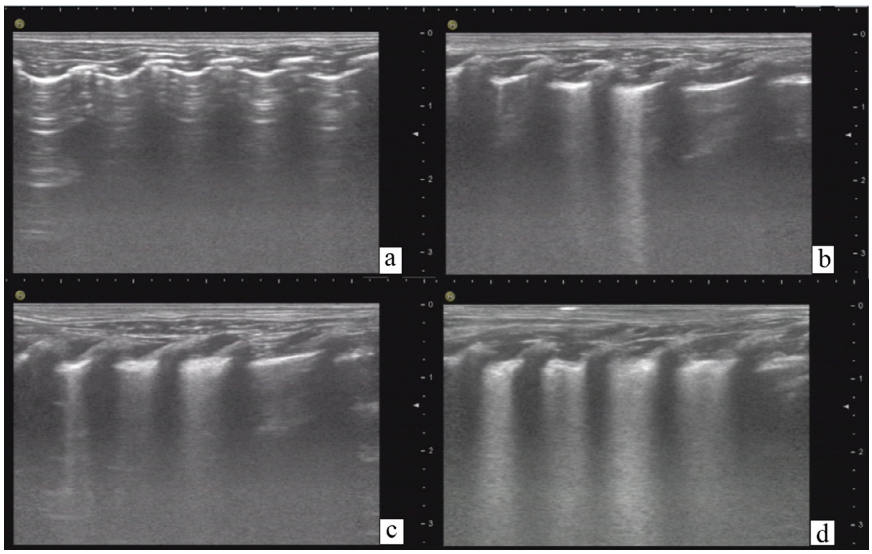

Fig. 1. Ultrasound images of the lungs. (a) Control group; (b) mild group; (c) moderate group; (d) severe group. Only a few scattered B-line artifacts were detected in the control group, whereas a large number of diffuse B-line artifacts were detected in the pulmonary edema groups.

as the mean ± standard deviation (continuous random variable) or median (Quartile 1−Quartile 3) (discrete random variable). Comparisons among groups were done with a one-way analysis of variance (with variance) or Kruskal−Wallis *H*-test (with uneven variance) followed by a least significant difference *t*-test (with variance) or Games−Howell test (with uneven variance) between two groups. Spearman correlation analysis was used to analyze the relationship between BLA features and pH, PaO_2, $PaCO_2$, TNF-α, IL-1β, IL-6, IL-8, LC and W/D. p values <0.05 were considered to indicate statistical significance.

RESULTS

Features of BLA

Only a few (≤5) scattered BLA were detected in the control group, whereas a large number of diffused BLA (abutting BLA <3 mm apart) were detected bilaterally in the pulmonary edema groups (Fig. 1). The time of appearance of BLA decreased ($p < 0.05$) while the number of BLA increased ($p < 0.05$) dose dependently with OA treatment (Table 4).

Artery blood gas analysis

Arterial blood gas values were normal in the control group, while acidosis, hypoxemia and hypocapnia were observed in the pulmonary edema groups. Furthermore, pH, PaO_2 and $PaCO_2$ decreased with increasing doses of OA ($p < 0.05$; Fig. 2).

Levels of TNF-α, IL-1β, IL-6 and IL-8

Levels of TNF-α, IL-1 β, IL-6 and IL-8 significantly increased in the pulmonary edema groups compared with the control group ($p < 0.05$). Furthermore, levels of TNF-α, IL-1 β, IL-6 and IL-8 increased with increasing dose of OA ($p < 0.05$; Fig. 3).

Table 4. BLA, LC and lung W/D

Group	No. of BLA	Appearance of BLA (min)	LC	W/D
Control	1 (0−4.25)	>30	3.81 ± 0.15	3.39 ± 0.12
Mild	18 (16.25−24.5)*	6.90 ± 0.56*	5.37 ± 0.11*	4.08 ± 0.15*
Moderate	36.5 (32.75−40.25)*,†	4.86 ± 0.33*,†	5.82 ± 0.15*,†	4.59 ± 0.09*,†
Severe	65.5 (57−67)*,†,‡	2.33 ± 0.62*,†,‡	6.58 ± 0.25*,†,‡	5.34 ± 0.16*,†,‡

BLA = B-line artifacts; LC = lung coefficient; W/D = wet weight-to-dry weight ratio
Time of appearance of BLA decreased while number of BLA, LC and lung W/D increased dose dependently on OA:
* $p<0.05$ versus control group;
† $p<0.05$ versus Mild group;
‡ $p<0.05$ versus moderate group.

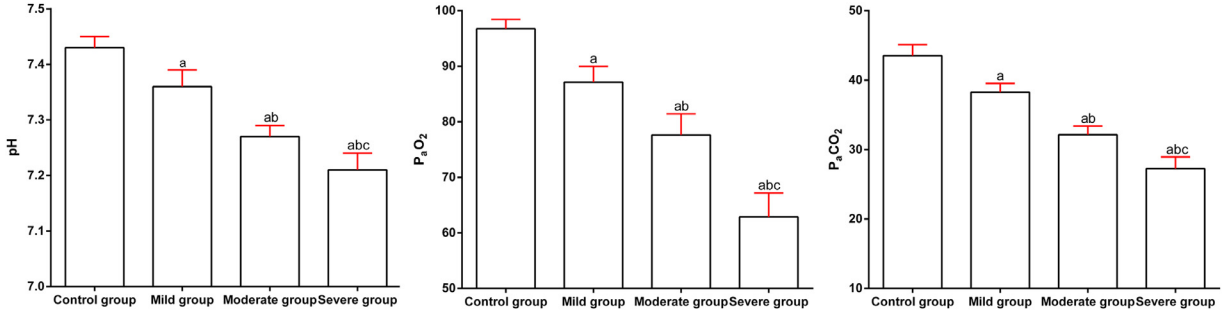

Fig. 2. Measurement of blood pH, PaO_2 and $PaCO_2$. Values of pH, PaO_2 and $PaCO_2$ decreased with increasing dose of OA. [a]$p < 0.05$ versus control group. [b]$p < 0.05$ versus mild group. [c]$p < 0.05$ versus moderate group.

Histologic features of the lung tissues

Lung tissues in the control group were a uniform pale pink color, whereas those in the pulmonary groups were a dark color. Moreover, enlarged volume, swelling, congestion, bleeding and uneven distribution of lung tissue were observed in the pulmonary edema groups (Fig. 4).

Alveolar structure in the control group was intact with no inflammation, hemorrhage, edema, atelectasis or necrosis. Alveoli were ruptured and fused in the pulmonary edema groups. In addition, edema fluid in the alveolar cavity and neutrophil infiltration and hemorrhage in alveoli and the interstitial space were observed in the pulmonary edema groups (Fig. 5).

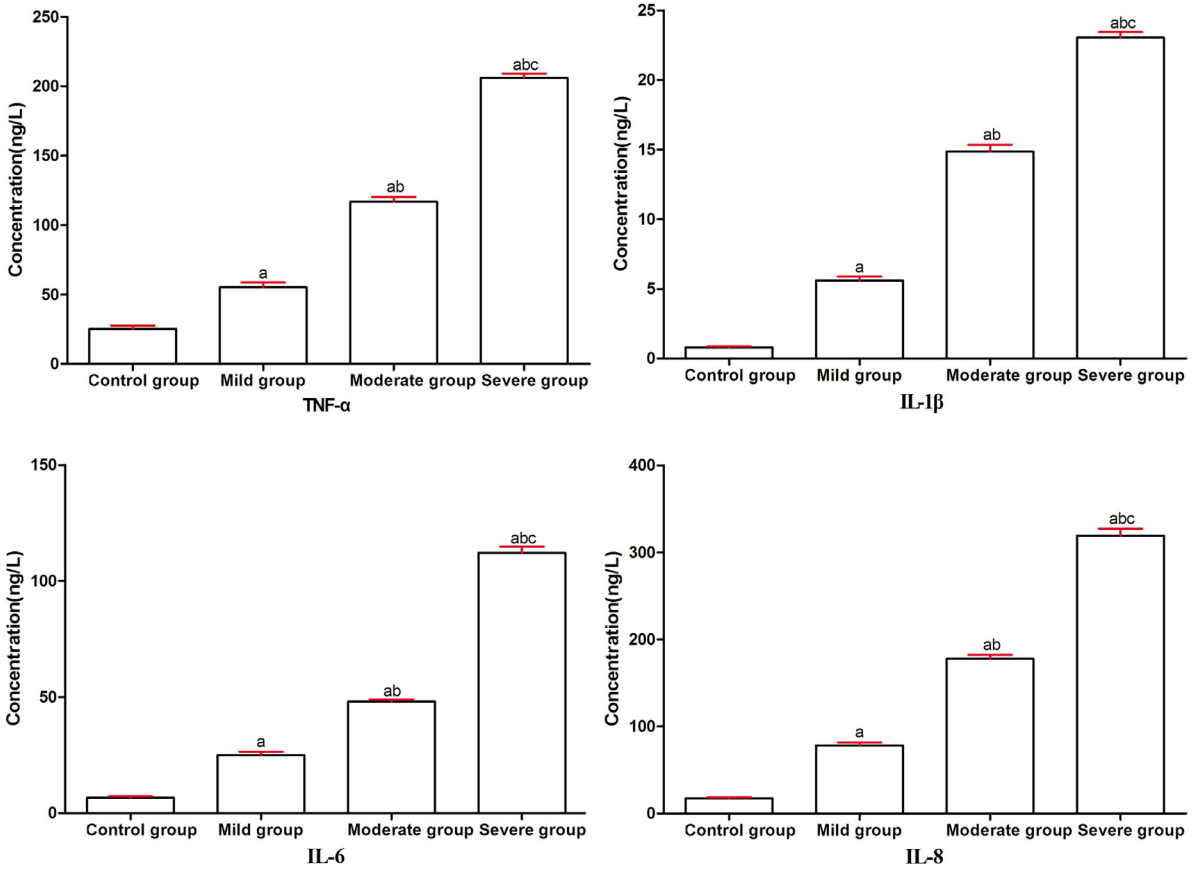

Fig. 3. Levels of blood inflammatory factors. Levels of TNF-α, IL-1β, IL-6 and IL-8 increased dose-dependently on oleic acid. [a]$p < 0.05$ versus control group. [b]$p < 0.05$ versus mild group. [c]$p < 0.05$ versus moderate group. TNF = tumor necrosis factor; IL – interleukin.

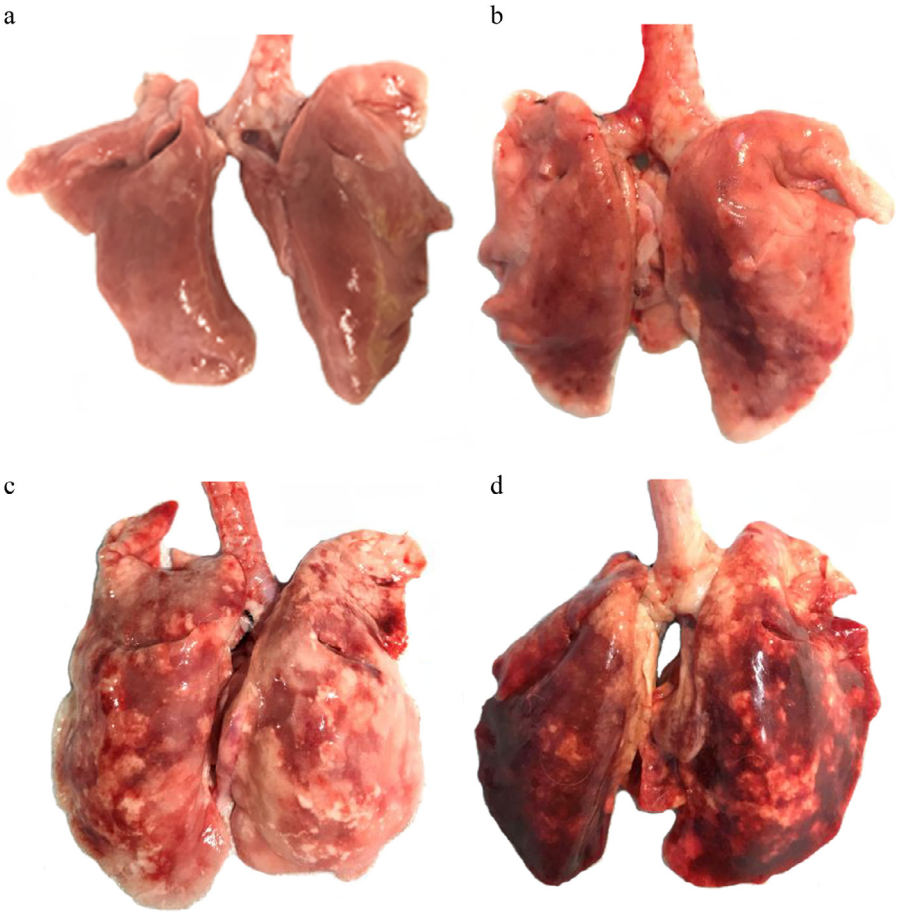

Fig. 4. Features of lung tissues. (a) Control group; (b) mild group; (c) moderate group; (d) severe group. The lung tissues in the control group (a) were a uniform pale pink color, while those in the pulmonary groups (b–d) were a dark color. Moreover, enlarged volume, swelling, congestion, bleeding and uneven distribution of the lung were observed in the pulmonary edema groups.

Compared with the control group, the pulmonary edema groups had increased LC and W/D values ($p < 0.05$) and aggravated lung histopathological manifestations ($p < 0.05$). Furthermore, LC, W/D and lung pathologic abnormalities increased dose dependently on OA ($p < 0.05$; Table 4).

Relationships between BLA and each variable

B-Line artifacts were linearly, negatively correlated with pH, PaO_2 and $PaCO_2$, while linearly, positively correlated with TNF-α, IL-1 β, IL-6, IL-8, LC and W/D ($p < 0.05$; Fig. 6).

BLA score and severity of pulmonary edema

Compared with the control group, the pulmonary edema groups had BLA and pulmonary edema severity scores that had increased dose dependently on OA ($p < 0.05$; Fig. 7). The BLA score was linearly, positively correlated with the severity of pulmonary edema ($r = 0.953$, $p < 0.05$).

Correlation between BLA-ev and lung pathologic abnormalities

The lung structure of the BLA-ev-free subregion was intact, whereas that of the BLA-ev-clustered subregion had ruptured and fused alveoli, edema fluid in the alveolar cavity, neutrophil infiltration and hemorrhage in alveoli and interstitial spaces. The severity of lung pathologic abnormalities increased with increasing number of BLA-ev ($p < 0.05$; Fig. 8). Furthermore, there was a linear positive correlation between features of BLA-ev and severity of lung pathologic abnormalities ($r = 0.936$, $p < 0.05$).

DISCUSSION

The presence of BLA strongly indicates the possibility of pulmonary edema formation. The sound power transmission coefficient is directly related to lung density. When pulmonary edema occurs, the gas/liquid ratio of the lung tissue decreases, the interval of the

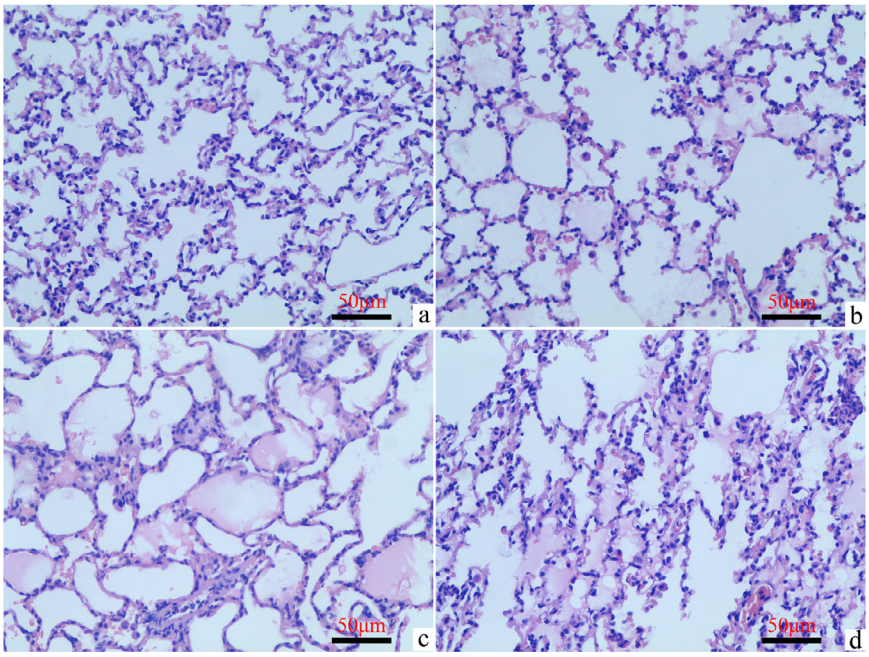

Fig. 5. Histologic examination of the lung tissues. (a) Control group; (b) mild group; (c) moderate group; (d) severe group. The alveolar structure in the control group was intact with no inflammation, hemorrhage, edema, atelectasis or necrosis (a). Alveoli were ruptured and fused in the pulmonary edema groups. In addition, edematous fluid in the alveolar cavity and neutrophil infiltration and hemorrhage in the alveoli and interstitial spaces were observed in the pulmonary edema groups (b–d).

pulmonary leaflets thickens and the difference in acoustic impedance between the gas and the liquid increases. Ultrasonic waves produce strong reverberation at the gas–liquid interface, and the sound beam makes a round trip back and forth to the thickened leaflet interval, leading to the formation of BLA. Thus, the presence of BLA indicates that interstitial spaces and alveoli are being filled with fluid or pulmonary edema formation (especially abutting BLA <3 mm apart). Therefore, the severity of pulmonary edema can be assessed on the basis of BLA features to some extent. Most previous studies on the tools used for diagnosis of pulmonary edema have focused on the use of POCUS in the attempt to make an accurate early quantitative diagnosis (Wang et al. 2018). However, POCUS might not reflect the severity of lung pathologic abnormalities accurately, and the correlation between features of BLA and severity of pulmonary edema has not been established. The present study indicated that the severity of the hypoxic and acid–base imbalance and the severity of inflammation can be assessed using BLA features, and the severity of lung pathologic abnormalities can be assessed based on the features of BLA-ev in the condition of pulmonary edema. What's more, BLA can be completed in a few minutes (Zanobetti et al. 2017), suggesting that POCUS can significantly reduce the time for diagnosis of pulmonary edema.

A rabbit OA-induced pulmonary edema model was used in this study. Scales rating the features of BLA and the severity of pulmonary edema were designed, and the features of BLA and severity of pulmonary edema were scored. The relationship between these two scores was analyzed. In addition, the relationship between features of BLA-ev and degree of the lung pathologic abnormalities was analyzed. In this way, we investigated the value of POCUS in making an early quantitative assessment of the severity of pulmonary edema.

Arterial blood gas changes reflect the ventilation and gas exchange function of the lung and the severity of acid–base imbalance (Dreher et al. 2019). In this study, shortness of breath and cyanosis developed quickly, and a pink foam-like liquid emerged from the nasal and oral cavity after injection of OA. Arterial blood gas analysis revealed that pH, PaO_2 and $PaCO_2$ decreased, indicating acidosis, hypoxemia and hypocapnia, respectively. Furthermore, because pH, as well as PaO_2 and $PaCO_2$, is negatively correlated with the number of BLA, the severity of hypoxia and acid–base imbalance in pulmonary edema can be assessed based on the number of BLA.

Inflammatory cytokines, such as TNF-α, IL-1 β, IL-6 and IL-8, which were secreted rapidly under the stimulation of inflammatory injury initiation factors, can cause acute injury to the lung tissues by activating cascades of

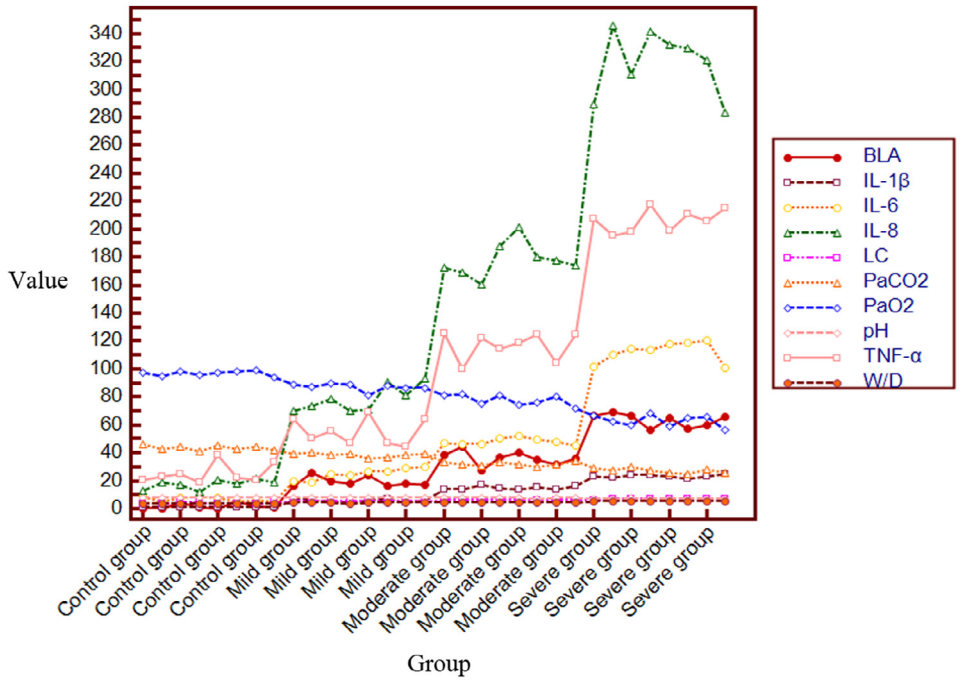

Fig. 6. Correlation between BLA and each variable. BLA were negatively correlated with pH, PaO_2 and $PaCO_2$, and positively correlated with TNF-α, IL-1 β, IL-6, IL-8, LC and W/D. BLA = B-line artifacts; TNF = tumor necrosis factor; IL = interleukin; LC = lung coefficient; W/D = wet weight-to-dry weight ratio.

inflammation (Butt et al. 2016). TNF-α, secreted mainly by activated macrophages and neutrophils, is a kind of endogenous inflammatory factor that is released first and leads to the secretion of inflammatory mediators such as IL-1 β, IL-6 and IL-8 in inflammatory reactions (Suzuki et al. 2013). TNF-α can promote acute injury to lung tissues by increasing the injury and autophagy of lung vascular endothelial cells, inhibiting the formation of pulmonary surfactant and causing paralysis of the diaphragm (Malaviya et al. 2017). IL-1β, the main promoter of the cellular inflammatory factor network (Mangan et al. 2018), is rapidly secreted by the induction of TNF-α and synergizes with TNF-α to further aggravate injury of lung tissues. The actions of IL-1β and TNF-α increase chemotaxis and activation of the neutrophils, stimulate the secretion of inflammatory mediators and oxygen free radicals by the pulmonary vascular endothelial cells and increase the permeability of the pulmonary vascular system by activating the coagulation system and inhibiting the fibrinolytic system in the early stage of lung inflammatory reactions (Howrylak and Nakahira 2017; Malaviya et al. 2017). IL-6 and IL-8, secreted mainly by lymphocytes, macrophages and endothelial cells, play an important role in the formation and development of acute inflammatory reactions in lung tissue (Krabbe et al. 2018; Rose-John 2018). Therefore, under the stimulation of the inflammatory injury initiation factors, TNF-α and IL-1β are rapidly secreted by lung tissues. IL-6 and IL-8 are subsequently secreted and activate the inflammatory cascades through the synergistic induction of TNF-α and IL-1β. Neutrophils accumulate in lung tissues, inflammatory mediators are released and inflammatory reaction effector cells are activated, which cause acute injury to the lung tissues and lead to the formation of pulmonary edema (Zhang et al. 2013; Kapur et al. 2015). In addition, studies have found that the levels of inflammatory factors in serum, such as TNF-α, IL-1 β, IL-6 and IL-8, parallel the severity of pulmonary edema (Li et al. 2018). Consistent with previous studies, levels of serum TNF-α, IL-1 β, IL-6 and IL-8 were significantly increased after injection of OA and increased gradually with increasing doses of OA, Moreover, this study found that levels of TNF-α, IL-1 β, IL-6 and IL-8 were positively correlated with the number of BLA. Therefore, to some extent, the severity of the inflammatory reactions of the lung tissues can be assessed by the number of BLA.

Lung histopathology is the gold standard for diagnosing and assessing the severity of pulmonary edema (Han et al. 2018), and LC and W/D are two important indicators in determining the severity of pulmonary edema (Chen et al. 2014). As described in the literature, this study found that lung pathologic abnormalities, LC and W/D all increased gradually with increasing dose of OA. Furthermore, lung histopathology, LC and W/D were found to be positively correlated with the number of BLA. However, lesions of the lung are unevenly

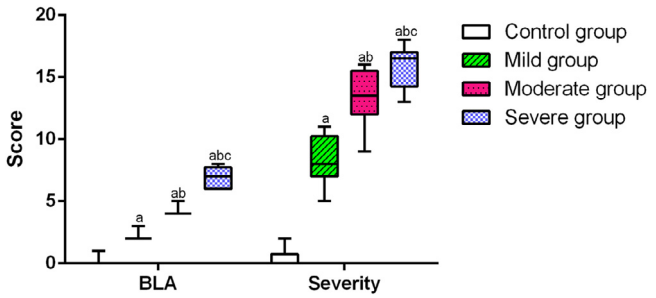

Fig. 7. BLA-ev score and severity of pulmonary edema. BLA score and severity of pulmonary edema increased dose dependently on oleic acid. [a]$p < 0.05$ versus control group. [b]$p < 0.05$ versus mild group. [c]$p < 0.05$ versus moderate group. BLA-ev = *ex vivo* B-line artifacts.

distributed because of gravity; thus, BLA tend to be gravitationally dependent. Therefore, the number of BLA in different subregions of the lung also differs (Irwin and Cook 2016). At present, there is no research focusing on how to choose the part of the lung for H&E staining based on the features of BLA. Therefore, the exact relationship between features of BLA and severity of the abnormality of the lung histopathological manifestations remains unknown. In this study, the lung was divided into subregions based on the features of BLA-ev, and lung pathologic abnormalities of each subregion were separately assessed. Our results indicated that although LC and W/D were the same, the degree of lung pathologic abnormalities increased with increasing number of BLA-ev. Furthermore, there is a positive correlation between the features of BLA-ev and the severity of lung pathologic abnormalities, suggesting that BLA-ev reflect the severity of lung pathologic abnormalities Therefore, the features of BLA can be used to assess the severity of lung histopathological abnormalities.

Although there are some limitations to this study (*i.e.,* the correlation between features of BLA and severity of lung pathologic abnormalities is still unclear and the number of rabbits in each group was limited), the findings of this study suggest the early quantitative assessment value of POCUS in pulmonary edema. The choice of which lung should be used for W/D or histologic analysis was not random in this study; thus, it may have generated

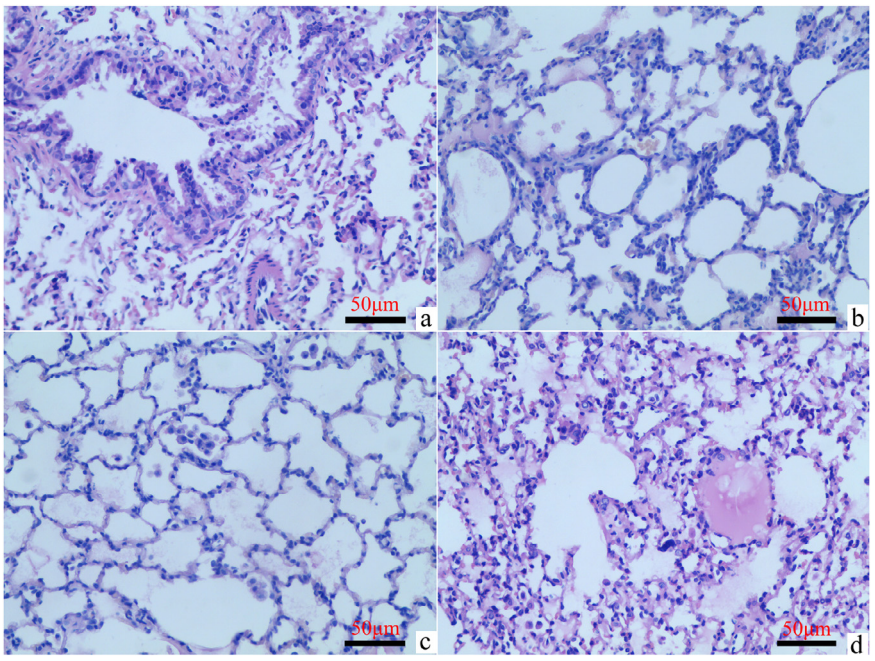

Fig. 8. Histologic images of lung tissues in different subregions. (a) free subregion; (b) rare-clustered subregion; (c) dense-clustered subregion; (d) confluent-clustered subregion. The lung structure of the BLA-ev-free subregion was intact (a), whereas that of the BLA-ev-clustered subregion had ruptured and fused alveoli, edematous fluid in the alveolar cavity and neutrophil infiltration and hemorrhage in alveoli and interstitial spaces (b–d). BLA-ev = *ex vivo* B-line artifacts.

some systematic bias. Lung tissue specimen biopsy *via* percutaneous lung puncture under the guidance of POCUS is in progress. It will not take long to solve the limitations described above.

CONCLUSIONS

Taken together, our findings indicate that POCUS is a promising novel method for the early quantitative assessment of the severity of pulmonary edema.

Acknowledgments—This research was supported by the Research Project of Science and Technology Department of Fujian Province, China (Grant 2018 J01288), the Youth Research Project of Health and Family Planning Commission of Fujian Province, China (Grants 2018-1-62 and 2018-2-23) and the Research Project of Collaborative Innovation Center for Maternal and Infant Health Service Application Technology (Grant XJM1802).

Conflict of interest disclosure—All authors declare that there is no conflict of interests regarding the publication of this article.

REFERENCES

Assaad S, Kratzert WB, Shelley B, Friedman MB, Perrino A, Jr. Assessment of pulmonary edema: principles and practice. J Cardiothorac Vasc Anesth 2018;32:901–914.

Butt Y, Kurdowska A, Allen TC. Acute lung injury: A clinical and molecular review. Arch Pathol Lab Med 2016;140:345–350.

Campbell SJ, Bechara R, Islam S. Point-of-care ultrasound in the intensive care unit. Clin Chest Med 2018;39:79–97.

Chen L, Zhao L, Zhang C, Lan Z. Protective effect of *p*-cymene on LPS induced acute lung injury in mice. Inflammation 2014;37:358–364.

Dietrich CF, Mathis G, Blaivas M, Volpicelli G, Seibel A, Wastl D, Atkinson NS, Cui XW, Fan M, Yi D. Lung B-line artefacts and their use. J Thorac Dis 2016;8:1356–1365.

Dreher M, Daher A, Keszei A, Marx N, Müller T, Cornelissen C, Brandenburg V. Whole body plethysmography and blood gas analysis in patients with acute myocardial infarction undergoing percutaneous coronary intervention. Respiration 2019;97:24–33.

Furue S, Kuwabara K, Mikawa K, Nishina K, Shiga M, Maekawa N, Ueno M, Chikazawa Y, Ono T, Hori Y, Matsukawa A, Yoshinaga M, Obara H. Crucial role of group IIA phospholipase A(2) in oleic acid-induced acute lung injury in rabbits. Am J Respir Crit Care Med 1999;160:1292–1302.

Gutierrez M, Salaffi F, Carotti M, Tardella M, Pineda C, Bertolazzi C, Bichisecchi E, Filippucci E, Grassi W. Utility of a simplified ultrasound assessment to assess interstitial pulmonary fibrosis in connective tissue disorders—Preliminary results. Arthritis Res Ther 2011;13:R134.

Han CH, Guan ZB, Zhang PX, Fang HL, Li L, Zhang HM, Zhou FJ, Mao YF, Liu WW. Oxidative stress induced necroptosis activation is involved in the pathogenesis of hyperoxic acute lung injury. Biochem Biophys Res Commun 2018;495:2178–2183.

Harvey S, Harrison DA, Singer M, Ashcroft J, Jones CM, Elbourne D, Brampton W, Williams D, Young D, Rowan K, PAC-Man Study Collaboration. Assessment of the clinical effectiveness of Pulmonary Artery Catheters in Management of Patients in Intensive Care (PAC-Man): A randomized controlled trial. Lancet 2005;366:472–477.

Howrylak JA, Nakahira K. Inflammasomes: Key mediators of lung immunity. Annu Rev Physiol 2017;79:471–494.

Irwin Z, Cook JO. Advances in point-of-care thoracic ultrasound. Emerg Med Clin North Am 2016;34:151–157.

Jambrik Z, Gargani L, Adamicza A, Kaszaki J, Varga A, Forster T, Boros M, Picano E. B-Lines quantify the lung water content: A lung ultrasound versus lung gravimetry study in acute lung injury. Ultrasound Med Biol 2010;36:2004–2010.

Kapur R, Kim M, Shanmugabhavananthan S, Liu J, Li Y, Semple JW. C-Reactive protein enhances murine antibody-mediated transfusion-related acute lung injury. Blood 2015;126:2747–2751.

Krabbe J, Ruske N, Braunschweig T, Kintsler S, Spillner JW, Schröder T, Kalverkamp S, Kanzler S, Rieg AD, Uhlig S, Martin C. The effects of hydroxyethyl starch and gelatine on pulmonary cytokine production and oedema formation. Sci Rep 2018;8:5123.

Li DK, Liu DW, Long Y, Wang XT. Use of lung ultrasound to assess the efficacy of an alveolar recruitment maneuver in rabbits with acute respiratory distress syndrome. J Ultrasound Med 2015;34:2209–2215.

Li K, He Z, Wang X, Pineda M, Chen R, Liu H, Ma K, Shen H, Wu C, Huang N, Pan T, Liu Y, Guo J. Apigenin C-glycosides of *Microcos paniculata* protects lipopolysaccharide induced apoptosis and inflammation in acute lung injury through TLR4 signaling pathway. Free Radic Biol Med 2018;124:163–175.

Lindholm P, Swenson ER, Henry G, Guo HH. From ocean deep to mountain high: Similar CT findings in immersion and high altitude pulmonary edema. Am J Respir Crit Care Med 2018;198:1088–1089.

Malaviya R, Laskin JD, Laskin DL. Anti-TNFα therapy in inflammatory lung diseases. Pharmacol Ther 2017;180:90–98.

Mangan MSJ, Olhava EJ, Roush WR, Seidel HM, Glick GD, Latz E. Targeting the NLRP3 inflammasome in inflammatory diseases. Nat Rev Drug Discov 2018;17:588–606.

McLario DJ, Sivitz AB. Point-of-care ultrasound in pediatric clinical care. JAMA Pediatr 2015;169:594–600.

Mrozek JD, Smith KM, Bing DR, Meyers PA, Simonton SC, Connett JE, Mammel MC. Exogenous surfactant and partial liquid ventilation: Physiologic and pathologic effects. Am J Respir Crit Care Med 1997;156(4, Pt 1):1058–1065.

Rose-John S. Interleukin-6 family cytokines. Cold Spring Harb Perspect Biol 2018;10(2):pii a028415.

Soldati G, Inchingolo R, Smargiassi A, Sher S, Nenna R, Inchingolo CD, Valente S. Ex vivo lung sonography: Morphologic−ultrasound relationship. Ultrasound Med Biol 2012;38:1169–1179.

Soldati G, Smargiassi A, Inchingolo R, Sher S, Nenna R, Valente S, Inchingolo CD, Corbo GM. Lung ultrasonography may provide an indirect estimation of lung porosity and airspace geometry. Respiration 2014;88:458–468.

Suzuki J, Hamada E, Shodai T, Kamoshida G, Kudo S, Itoh S, Koike J, Nagata K, Irimura T, Tsuji T. Cytokine secretion from human monocytes potentiated by P-selectin-mediated cell adhesion. Int Arch Allergy Immunol 2013;160:152–160.

Volpicelli G, Elbarbary M, Blaivas M, Lichtenstein DA, Mathis G, Kirkpatrick AW, Melniker L, Gargani L, Noble VE, Via G, Dean A, Tsung JW, Soldati G, Copetti R, Bouhemad B, Reissig A, Agricola E, Rouby JJ, Arbelot C, Liteplo A, Sargsyan A, Silva F, Hoppmann R, Breitkreutz R, Seibel A, Neri L, Storti E, Petrovic T. International evidence-based recommendations for point-of-care lung ultrasound. Intensive Care Med 2012;38:577–591.

Wang Y, Shen Z, Lu X, Zhen Y, Li H. Sensitivity and specificity of ultrasound for the diagnosis of acute pulmonary edema: A systematic review and meta-analysis. Med Ultrason 2018;1:32–36.

Ware LB, Matthay MA. Acute pulmonary edema. N Engl J Med 2005;353:2788–2796.

Warren MA, Zhao Z, Koyama T, Bastarache JA, Shaver CM, Semler MW, Rice TW, Matthay MA, Calfee CS, Ware LB. Severity scoring of lung oedema on the chest radiograph is associated with clinical outcomes in ARDS. Thorax 2018;73:840–846.

Zanobetti M, Scorpiniti M, Gigli C, Nazerian P, Vanni S, Innocenti F, Stefanone VT, Savinelli C, Coppa A, Bigiarini S, Caldi F, Tassinari I, Conti A. Point-of-care ultrasonography for evaluation of acute dyspnea in the ED. Chest 2017;151:1295–1301.

Zhang H, Neuhöfer P, Song L, Rabe B, Lesina M, Kurkowski MU, Treiber M, Wartmann T, Regnér S, Thorlacius H, Saur D, Weirich G, Yoshimura A, Halangk W, Mizgerd JP, Schmid RM, Rose-John S, Algül H. IL-6 trans-signaling promotes pancreatitis-associated lung injury and lethality. J Clin Invest 2013;1:1019–1031.